Dissolution and precipitation processes governing the hydration heat development in tunnel cements: Green's function-based estimation of heat release in modified calorimetric tests

Hermann Höld, Bernhard Pichler, Christian Hellmich
Institute for Mechanics of Materials and Structures, TU Wien (Vienna University of Technology), Vienna, Austria

Helmut Rechberger, Philipp Aschenbrenner
Institute of Water Quality and Resource Management, TU Wien (Vienna University of Technology), Vienna, Austria

ABSTRACT: Cement hydration in freshly installed NATM-linings may imply significant temperature rises, as has been monitored during the advance of the Granitztal tunnel, as part of the high-capacity railway corridor linking the Baltic and Adriatic regions. These temperature rises affect the overall thermo-chemo-mechanical behavior of the lining and its surroundings, which can be elucidated by a coupled analysis method combining the laws of thermodynamics for chemically reactive media with advanced constitutive modeling and structural mechanics. A key material property entering such computations is the hydration heat per mass of cement, which is the focus of the present contribution. We present a modified calorimetry test where the absolute temperature is measured directly at the boundary of the hydrating cement paste sample prepared in accordance with the provisions at the Granitztal tunnel. This modified calorimetry test give access to the instant heat release rate arising from the hydration process.

Keywords: Tunnel, Cement, Hydration, Calorimetry, First Peak.

1 INTRODUCTION

The temperature evolution measured in a calorimetric test is an important and easily accessible fingerprint of the chemical reactions between cement and water, referred to as hydration. More precisely, it is customary to translate the temperature evolution into a heat release rate, and to relate the latter to the evolution of a hydration degree (Ulm & Coussy 1996 and Hellmich et al. 1999), which, in turn, governs important mechanical properties, such as the compressive strength of cement paste and concrete (Pichler & Hellmich 2011 and Königsberger et al. 2018). The latter are key input for the thermo-chemo-mechanical analyses of concrete and shotcrete tunnel shells (Hellmich et al. 2001 and Scharf et al. 2022).

However, hydration remains a very complex process, even in the very well-defined conditions of an isothermal differential calorimeter. Accordingly, key assumptions concerning the translation from temperature into heat release, the key indicator of hydration kinetics, deserve deeper scrutiny, and this is exactly the focus of the present contribution. Accordingly, we here present the results of calorimetric tests, interpret them in light of recent insight into hydration reactions (Nicoleau et al.

2013 and Nicoleau & Nonat 2016), and provide an improved evaluation method resting on the Green's function-based solution of the transient heat generation and conduction problem.

2 CALORIMETRY – BASIC FEATURES OF HYDRATION

The focus of the present contribution is an improved quantitative evaluation of isothermal calorimetric tests, which we performed by means of an isothermal differential calorimeter of the type ToniCAL Trio 7339, produced by Toni Technik Baustoffprüfsysteme GmbH. From the temperature difference between hydrating and chemically inert sample, ΔT, see Figure 1, the total heat flow leaving the hydrating sample, q_{tot}, is determined according to:

$$q_{tot} = CF \cdot \Delta T \tag{1}$$

whereby the calibration factor *CF* was determined by a calorimeter-specific calibration test.

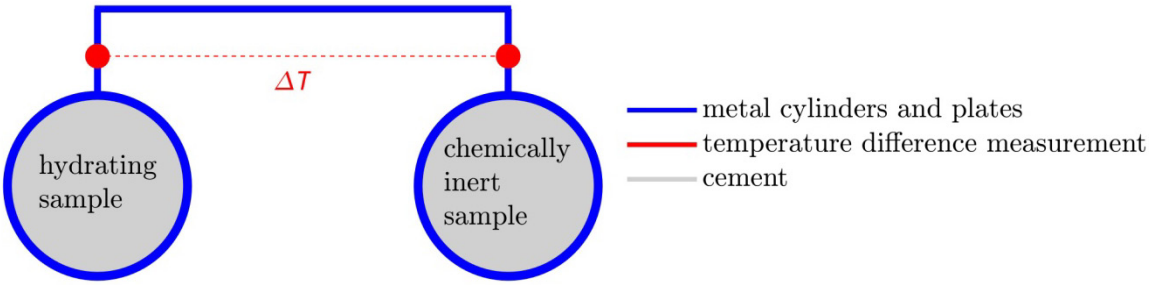

Figure 1. Schematic cross-section of the calorimeter, comprising two metal cylinders hosting a hydrating and an inert sample, respectively, and being thermally connected by metal plates, across which the temperature difference ΔT is measured.

In Figure 2, the total heat flow leaving the hydrating sample, q_{tot}, is shown for a sample of the CEM I cement with a water-to-cement ratio of 0.44, as utilized in the Granitztal tunnel (Bauer et al. 2016, Gschwandtner et al. 2017, Moritz et al. 2021). The corresponding sample, with a height of 55 mm and a radius of b = 8 mm, is depicted in Figure 3.

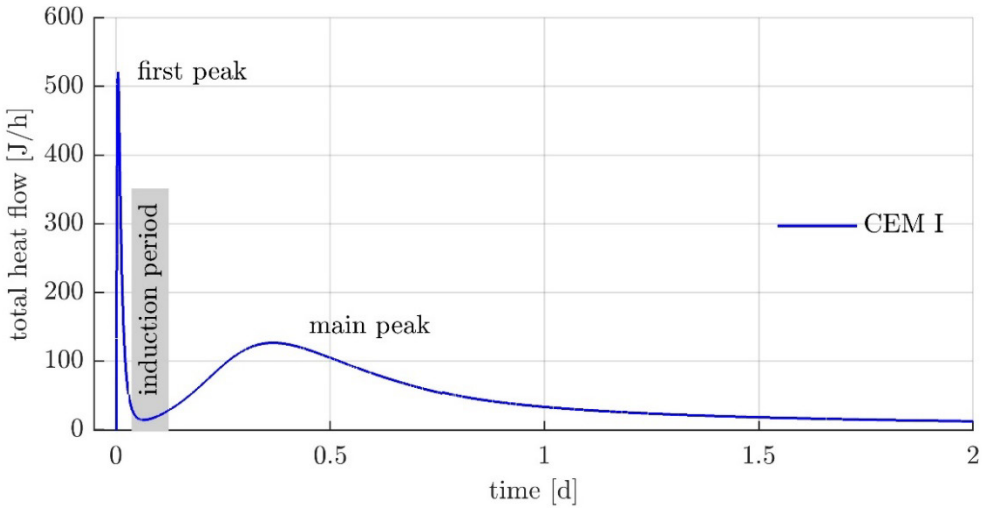

Figure 2. Total heat flow leaving the hydrating sample of the tested CEM I cement. The curve is characteristic for cement and shows the first peak, the induction period, and the main peak.

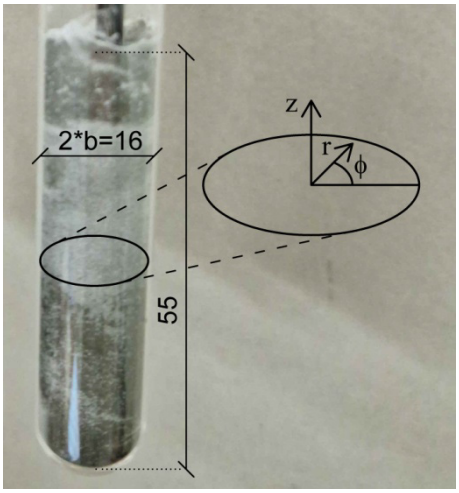

Figure 3. A sample with hardened cement with its cylindrical coordinate system. The dimensions are in millimeters.

We observe the following typical characteristics of the heat provided by the hydrating sample: A first, high conduction peak, indicating massive heat generation at the beginning of the hydration, is followed, after a so-called induction period, by considerably lower and wider main conduction peak. In order to understand the underlying causes of these peaks, Nicoleau & Nonat (2016) have conducted a systematic review and evaluation of ion concentration measurements in solutions and hardening cement, provided by methods such as inductively coupled plasma (ICP) spectrometry (Rothstein et al. 2002 and Nicoleau et al. 2013), colorimetry (Brown et al. 1984), X-ray diffraction, thermogravimetric analysis (TGA) (Lothenbach and Winnefeld, 2006), and calorimetry (Deschner et al. 2012). They showed that the first peak results from the dissolution process of clinker coming together with an increasing ionic saturation of water (Nicoleau et al. 2013), while the main peak relates to the coupled dissolution-precipitation process, in which clinker (mainly: tricalcium silicate) is dissolved and calcium-silicate-hydrate and portlandite precipitate (Nicoleau & Nonat 2016).

3 CLASSICAL ESTIMATION OF HEAT RELEASE RATE - ASSUMPTION OF STATIONARITY

The classical estimation is based on the assumption that the internal energy remains constant over the calorimetric test so that the first law of thermodynamics implies the total heat leaving the hydrating sample, as referred to in Section 2, is equal to the heat generation rate of the hydrating sample, g_{tot}. Diving the latter by the mass of the hydrating sample results in the specific heat release rate as depicted in Figure 5.

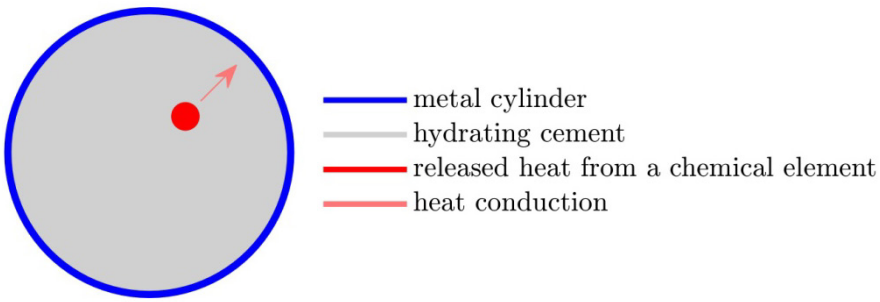

Figure 4. Coupled heat generation-conduction problem in the hydrating sample (Hellmich et al. 1999): the heat released from material volume ("chemical element") leads to (i) internal energy increase due to local temperature rise, and (ii) heat flow from the material volume to its surrounding.

4 GREEN'S FUNCTION APPROACH CONSIDERING INSTATIONARITY: IMPROVED ESTIMATE OF HEAT RELEASE RATE

For the improved estimation of the heat release rate, the change of internal energy is considered; namely in terms of the heat capacity multiplied with the local temperature rise; to be balanced by local heat generation and local heat flow as seen in Figure 4. In order to get access to the absolute value of the temperature, rather than to only the temperature difference between the metal cylinders seen in Figure 1, an additional temperature sensor was installed in the calorimeter, close to the metal cylinder hosting the hydrating sample.

From a mathematical viewpoint, we resort to the so-called heat conduction equation, which combines the first law of thermodynamics with Fourier's heat conduction law while restricting internal energy effects to heat capacity phenomena, and we solve the latter for an infinitely long cylinder, with a radial symmetric, uniform distribution of radial heat flow vectors across its outer surface,

$$\boldsymbol{q} = \boldsymbol{e}_{\mathrm{r}} \frac{q_{tot}}{2\pi bh} \,. \tag{2}$$

Under these conditions, the heat conduction equation reads as (Hahn & Özişik 2012):

$$\frac{\partial^2 T}{\partial r^2} + \frac{1}{r}\frac{\partial T}{\partial r} + \frac{g}{k} = \frac{1}{\alpha}\frac{\partial T}{\partial t} \qquad in\ 0 \le r < b, t > 0 \tag{3}$$

$$\begin{aligned} &\text{BC1:} \quad T(r \to 0, t) \to \text{finite} \\ &\text{BC2:} \quad -k\frac{\partial T}{\partial r}(r = b, t) = f(t) \\ &\text{IC:} \quad T(r, t = 0) = F(r) \end{aligned} \tag{4}$$

where $T(r,t)$ is the temperature of the probe at position r and time t in °C, b is the radius of the probe in m, k is the thermal conductivity in W/mK, $\alpha = k/\rho c$ is the thermal diffusivity in m^2/s, ρ is the mass density in kg/m^3, c is the constant volume specific heat in J/kgK, $F(r)$ is the initial temperature (at time $t = 0$) and $g(r,t)$ is the volumetric rate of internal energy generation in W/m^3. The first boundary condition BC1 means that the temperature at the origin of the radial coordinate must have a finite value. The second boundary condition BC2 specifies the time-varying heat flow $f(t) = q_{tot} \,/\, 2\pi bh$ at the boundary of the sample. The initial condition IC will be described later.

Usually, the temperature $T(r,t)$ is the function to search for in a nonhomogeneous transient heat conduction problem according to the equations (3) and (4). The problem can be solved using Green's functions, and the temperature is calculated as follows (Hahn & Özişik 2012):

$$\begin{aligned} T(r,t) = & \int_{r'=0}^{b} G(r,t|r',\tau=0)F(r')r'\,\mathrm{d}r' \\ & + \frac{\alpha}{k}\int_{\tau=0}^{t}\int_{r'=0}^{b} G(r,t|r',\tau)g(r',\tau)\,r'\,\mathrm{d}r'\mathrm{d}\tau \\ & + \frac{\alpha}{k}\int_{\tau=0}^{t} G(r,t|b,\tau)f(\tau)\,b\,\mathrm{d}\tau\,, \end{aligned} \tag{5}$$

whereby the Green's function reads as:

$$G(r,t|r',\tau) = \frac{2}{b^2} + \frac{2}{b^2}\sum_{n=1}^{\infty}\frac{J_0(\lambda_n r')\,J_0(\lambda_n r)}{J_0^2(\lambda_n b)}e^{-\alpha\lambda_n^2 t}. \tag{6}$$

Usually equation (5) is used to calculate the temperature in the sample $T(r,t)$. However, here equation (5) is used to calculate the rate of volumetric heat generation $g(r,t)$, which corresponds to the heat release rate per mass g_ρ for a sample containing 10 g cement through $g_\rho(t) = g_{tot}/10 = \int g(r,t)\, dV/10$. Evaluation of equation (5) for $r = b$, setting the result equal to the measured temperature evolution, while considering an initially uniform temperature of $F(r) = 25°C$ and the heat flow $f(t)$ estimated through measured temperature difference according to equations (1) and (2), allows for estimation of $g(r,t)$, and subsequently, of the heat release rate per unit mass, see Figure 5.

We observe that the heat release peak due to cement dissolution is more than twice as large as classically estimated, and that the latter artificially retards the occurrence of the precipitation peak.

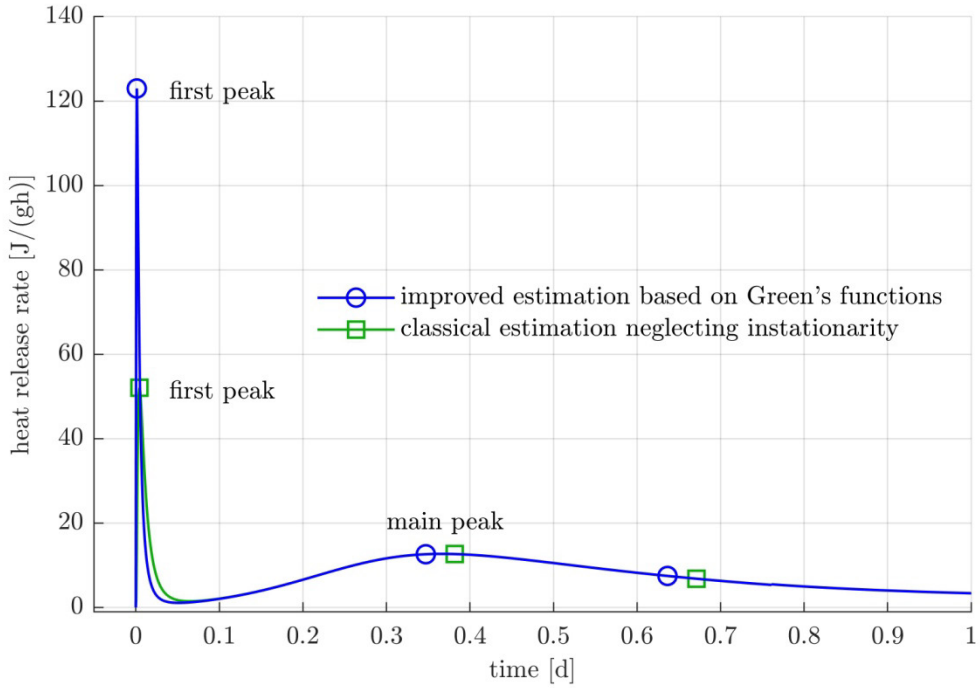

Figure 5. Comparison of the classical estimation of the heat release rate neglecting instationarity and the improved estimation of the heat release rate based on Green's functions of the tested CEM I cement.

5 CONCLUSIONS

Consideration of temperature instationarity due to heat capacity effects leads to a higher heat release peak due to cement dissolution and to an earlier occurrence of the heat peak due to hydrate precipitation, when compared to the classical estimation method neglecting the aforementioned effects. We expect this refined representation of the overall hydration process to further enhance the state-of-the-art in the micro-thermo-chemo-mechanics of concrete, as used in NATM tunnel monitoring by so-called hybrid methods (Pichler & Hellmich 2018). Future work will comprise validation of results by means of inductively coupled plasma – optical emission spectrometry (ICP-OES), as well as by temperature measurements on tunnel sites.

ACKNOWLEDGEMENTS

The authors gratefully acknowledge project FFG-COMET #882504 "Rail4Future: Resilient Digital Railway Systems to enhance performance".

REFERENCES

Bauer, J., Kohlböck, B., Moritz, B. & Zwittnig, G. 2016. The Granitztal tunnel chain - state of works on the second longest tunnel system on the Koralmbahn / Tunnelkette Granitztal – Stand der Arbeiten für das zweitlängste Tunnelsystem an der Koralmbahn. *Geomechanics and Tunnelling* 9 (5), pp. 416–427, Ernst & Sohn: Berlin.

Brown, P., Franz, E., Frohnsdorff, G. & Taylor, H. 1984. Analyses of the aqueous phase during early C_3S Hydration. *Cement and Concrete Research* 14. pp. 257-262.

Deschner, F., Winnefeld, F., Lothenbach, B., Seufert, S., Schwesig, P., Dittrich, S., Goetz-Neunhoeffer, F. & Neubauer, J. 2012. Hydration of Portland cement with high replacement by siliceous fly ash. *Cement and Concrete Research* 42. pp. 1389-1400.

Gschwandtner, G. G., Kahn, U., Kohlböck, B., Moritz, B. & Wagner. S. 2017. Granitztal tunnel chain - Experience from the construction of the Langer Berg Tunnel and challenges in the anhydrite zone. *Geomechanics and Tunnelling* 10 (6), pp 730–739, Ernst & Sohn: Berlin.

Hahn, D. W. & Özişik, M. N. Heat Conduction, 3rd Edition. 2012. *John Wiley & Sons, Inc.*

Hellmich, C., Ulm, F.-J. & Mang, H. 1999. Consistent linearization in Finite Element analysis of coupled chemo-thermal problems with exo- or endothermal reactions. *Computational Mechanics* 24, pp 238–244.

Hellmich, C., Mang, H. A. & Ulm, F.-J. 2001. Hybrid method for quantification of stress states in shotcrete tunnel shells: combination of 3D in situ displacement measurements and thermochemoplastic material law. *Computers & Structures* 79 (22), pp. 2103–2115.

Königsberger, M., Hlobil, M., Delsaute, B., Staquet, S., Hellmich, C. & Pichler, B. 2018. Hydrate failure in ITZ governs concrete strength: A micro-to-macro validated engineering mechanics model. *Cement and Concrete Research* 103, pp. 77-94.

Lothenbach, B. & Winnefeld, F. 2006. Thermodynamic modelling of the hydration of Portland cement. *Cement and Concrete Research* 36. pp. 209-226.

Moritz, B., Heissenberger, R., Schachinger, T. & Lienhart, W. 2021. Long-term monitoring of railway tunnels. *Geomechanics and Tunnelling* 14 (1), pp 35–46, Ernst & Sohn: Berlin.

Nicoleau, L., Nonat, A. & Perrey, D. 2013. The di- and tricalcium silicate dissolutions. *Cement and Concrete Research* 47. pp. 14-30.

Nicoleau, L. & Nonat, A. 2016. A new view on the kinetics of tricalcium silicate hydration. *Cement and Concrete Research* 86, pp. 1–11.

Pichler, B. & Hellmich, C. 2011 Upscaling quasi-brittle strength of cement paste and mortar: A multi-scale engineering mechanics model. *Cement and Concrete Research* 41, pp. 467-476

Pichler, B. & Hellmich, C. 2018. Hybrid methods for shotcrete and segmental linings tunnel shells – combining displacement and rotation measurements with computational multiscale mechanics. *Geomechanics and Tunnelling* 11 (3), pp 226–235. Ernst & Sohn: Berlin.

Rothstein, D., Thomas, J., Christensen, B. & Jennings, H. 2002. Solubility behavior of Ca-, S-, Al-, and Si-bearing solid phases in Portland cement pore solutions as a function of hydration time. *Cement and Concrete Research* 32. pp. 1663-1671.

Scharf, R., Pichler, B., Heissenberger, R., Moritz, B. & Hellmich, C. 2022. Data-driven analytical mechanics of aging viscoelastic shotcrete tunnel shells. *Acta Mechanica*, pp. 2989–3019

Ulm, F.-J. & Coussy, O. 1996. Strength growth as chemo-plastic hardening in early age concrete. *Journal of Engineering Mechanics* 122(12). pp. 1123–1132.